J. Phys.: Condens. Matter **8** (1996) 287–302. Printed in the UK

Transferability of a local pseudopotential based on solid-state electron density

Fernando Nogueira†, Carlos Fiolhais†, Jingsong He‡, John P Perdew‡ and Angel Rubio§

† Department of Physics, University of Coimbra, P3000 Coimbra, Portugal
‡ Department of Physics, Tulane University, New Orleans, LA 70118, USA
§ Department of Theoretical Physics, University of Valladolid, E-47011 Valladolid, Spain

Received 3 July 1995, in final form 14 November 1995

Abstract. Local electron–ion pseudopotentials fitted to dominant density parameters of the solid state (valence, equilibrium average electron density and interstitial electron density) have been constructed and tested for sixteen simple metals. Calculated solid-state properties present little evidence of the need for pseudopotential non-locality, but this need is increasingly evident as the pseudopotentials are transferred further from their solid-state origins. Transferability is high for Na, useful for ten other simple metals (K, Rb, Cs, Mg, Al, Ga, In, Tl, Sn, and Pb), and poor for Li, Be, Ca, Sr and Ba. In the bulk solid, we define a predictor of transferability and check the convergence of second-order pseudopotential perturbation theory for bcc Na. For six-atom octahedral clusters, we find that the pseudopotential correctly predicts self-compressions or self-expansions of bond length with respect to the bulk for Li, Na, Mg, and Al, in comparison with all-electron results; dimers of these elements are also considered. For the free atom, we examine the bulk cohesive energy (which straddles the atomic and solid-state limits), the atomic excitation energies and the atomic density. For the cohesive energy, we also present the results of the simpler stabilized jellium and universal-binding-energy-curve models. The needed non-locality or angular-momentum dependence of the pseudopotential has the conventional character, and is most strongly evident in the excitation energies.

1. Introduction and a summary of conclusions

The pseudopotential [1, 2, 3, 4], a weak effective interaction between a valence electron and an ion core, brings a useful simplification to condensed-matter physics and quantum chemistry, at some cost in accuracy. The simplest and least accurate pseudopotentials are local or multiplication operators $w(r)$, the same for all components of the electron's angular momentum. This locality is required for fair tests of density functional approximations [5] against more accurate many-body methods, and has a number of other practical advantages [6, 7]. Two of us have recently proposed a local pseudopotential (the individual 'evanescent-core pseudopotential' of [7]) fitted to three dominant density parameters of a simple metal: the valence z, the equilibrium average valence electron density

$$\bar{n} = \frac{3}{4\pi r_s^3} \tag{1}$$

and $\bar{n}_{int}$, the electron density averaged over the interstitial region between the surface of the polyhedral Wigner–Seitz cell and the inscribed sphere. Thus we have refined the 'stabilized jellium' [8, 9] and 'ideal metal' [10] models through the introduction of atomic structure.

0953-8984/96/030287+16$19.50

Our pseudopotential was constructed and tested for 16 simple metals in close-packed (fcc, hcp) or nearly close-packed (bcc) crystal structures. All calculations in [7] and in the present work employ the local spin-density approximation for exchange and correlation [5].

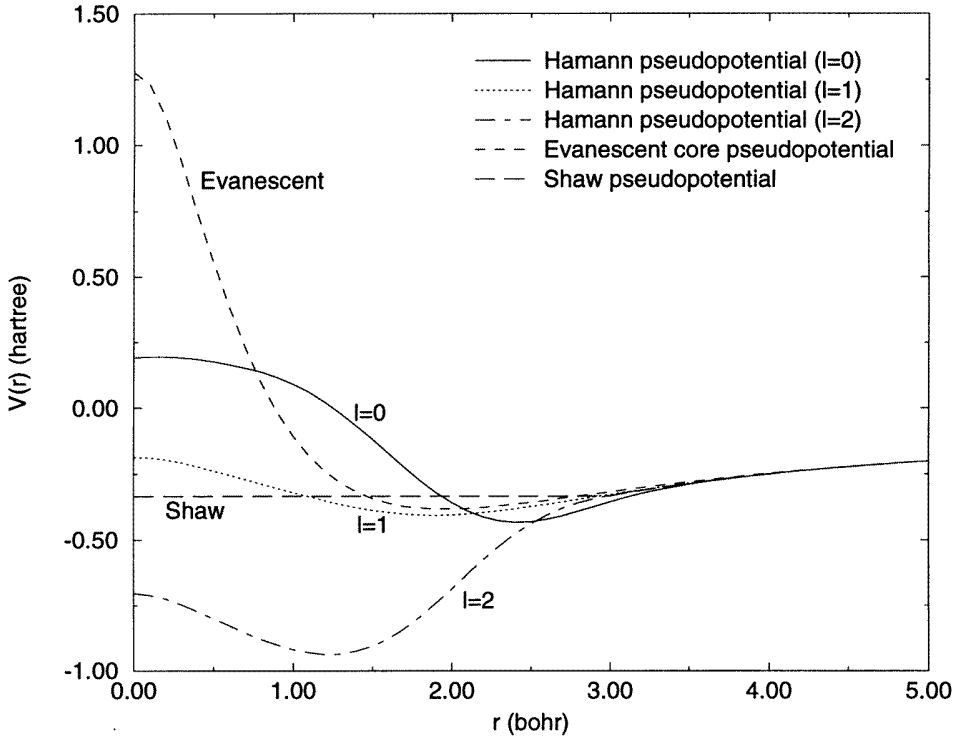

Figure 1. A comparison of Hamann's non-local pseudopotential [15] to the local Shaw [36] and evanescent-core [7] pseudopotentials for Na. The single parameter of the Shaw form was fitted [13] to the equilibrium average valence electron density $\bar{n}$.

Our local pseudopotential has definite advantages over the Ashcroft form [11], which fails to predict the bulk moduli correctly [12], and over the Ling–Gelatt form [13], which places the first zero of the Fourier transform $w(Q)$ incorrectly [13]. In fact, in our solid-state calculations [7] (bulk binding energies, bulk moduli and their pressure derivatives, chemical potentials, and structural energy differences), we found little evidence of any need for non-locality, except in our incorrect structural predictions for Ca, Sr and Ba (where it may be not so much non-locality as energy dependence [14] that is needed). Our local pseudopotential is in a sense optimized for the bulk solid-state environment.

Sodium is one of the metals for which a local pseudopotential can be expected to work well. Figure 1 compares our local pseudopotential for sodium with the non-local, norm-conserving pseudopotential of Hamann [15]. In valence and outer-core regions of space, the local pseudopotential provides a kind of average of the non-local pseudopotentials seen by s and p valence electrons; in the inner core, it is considerably 'harder' or more repulsive. The situation is very similar for Mg and Al.

In this work, we examine the extent to which our local pseudopotential can be transferred successfully from the solid state to other environments. It will be seen that the local pseudopotential is highly transferable for Na, usefully transferable for ten other metals (K,

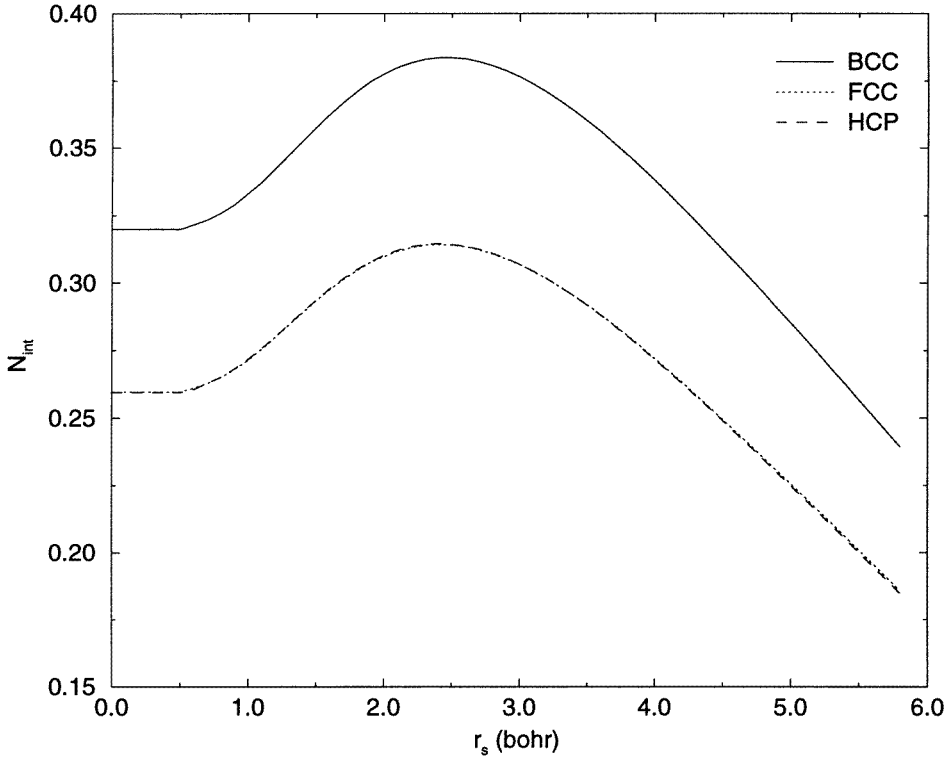

Figure 2. The number of interstitial valence electrons N_{int} versus the density parameter r_s for Na in three different structures (bcc, fcc and hcp). The fcc and hcp curves are almost identical. In the limit $r_s \to 0$, N_{int} tends to $z\Omega_{int}/\Omega_{WS}$, where Ω_{int} and Ω_{WS} are the interstitial and Wigner–Seitz cell volumes.

Rb, Cs, Mg, Al, Ga, In, Tl, Sn, and Pb), but poorly transferable for Li, Be, Ca, Sr and Ba. Moreover, the pattern of errors indicates a need for pseudopotential non-locality of the conventional type [1, 2, 3, 4], in which the short-range repulsive part of the potential is most repulsive for s electrons, less so for p, and still less for d (figure 1). We are not aware of any previous systematic study of this sort.

We begin in section 2 with a discussion of the solid state. We define a dimensionless quantity $(\bar{n}/\bar{n}_{int})\,\mathrm{d}\bar{n}_{int}/\mathrm{d}\bar{n}$, and show that a comparison of its pseudopotential and all-electron values, evaluated at the equilibrium r_s, can predict whether or not the pseudopotential is transferable for a given element. Because our solid-state energies are evaluated to second order in the pseudopotential, we examine the accuracy of this perturbation expansion. For bcc sodium we find that it is adequate.

In section 3, we compare pseudopotential and all-electron results for the cohesive energy and nearest-neighbour distance in six-atom octahedral clusters. The pseudopotential predicts a self-compression for Li_6, Na_6, and Al_6 clusters, in comparison with bulk nearest-neighbour distances, and a self-expansion for Mg_6. Taking all-electron results as our standard, the quantitative error is small. Dimers of these elements show greater pseudopotential errors.

The free-atom limit, a more radical change from the bulk solid environment, is studied in section 4, where we evaluate the bulk cohesive energies, the low-lying excitation energies [16] and the electron densities for the free atom. The bulk cohesive energies

Table 1. The average valence electron density $\bar{n} = 3/r\pi r_s^3$ and average interstitial valence electron density $\bar{n}_{int}$ for the simple metals. In the notation of [7], $\bar{n}_{int}/\bar{n} = N_{int}^I/N_{int}^U$, and $(\bar{n}/\bar{n}_{int})\ \mathrm{d}\bar{n}_{int}/\mathrm{d}\bar{n} = 1-(r_s/3N_{int}^I)\ \mathrm{d}N_{int}^I/\mathrm{d}r_s$. Local pseudopotential [7] and all-electron values of $\bar{n}$ and $\bar{n}_{int}$ agree at the equilibrium $\bar{n}$, by construction. The crystal structures used here are the conventional ones from [7], but the results are not sensitive to crystal structure. For example, $\bar{n}_{int}/\bar{n} = 1.06$ for fcc Na, 1.02 for bcc Mg, and 0.93 for bcc Al (when evaluated by either the pseudopotential perturbation or all-electron methods).

		$(\bar{n}/\bar{n}_{int})\ \mathrm{d}\bar{n}_{int}/\mathrm{d}\bar{n}$		
Metal	$\bar{n}_{int}/\bar{n}$	Pseudopotential	(error)	All-electron
Li	1.08	1.18	(+6%)	1.11
Na	1.07	1.18	(−2%)	1.20
K	1.11	1.19	(−3%)	1.22
Rb	1.11	1.19	(−4%)	1.23
Cs	1.12	1.19	(−1%)	1.20
Be	0.98	1.36	(+19%)	1.14
Mg	1.01	1.42	(+8%)	1.31
Ca	1.06	1.43	(+16%)	1.23
Sr	1.06	1.45	(+16%)	1.25
Ba	1.08	1.43	(+27%)	1.13
Al	0.91	1.51	(+8%)	1.40
Ga	0.72	1.63	(+10%)	1.48
In	0.76	1.63	(+6%)	1.54
Tl	0.68	1.70	(+19%)	1.43
Sn	0.67	1.74	(+22%)	1.43
Pb	0.62	1.81	(+23%)	1.47

Table 2. A comparison of perturbative and non-perturbative results for bcc Na using the same local pseudopotential (the individual evanescent-core pseudopotential of [7]). The perturbation expansion is carried to first order for the density, and to second order for the energy. The 'Non-perturbative A' and 'Non-perturbative B' calculations are evaluated at the density parameters r_s that minimize the perturbative and non-perturbative energies, respectively. The 'Non-perturbative C' results are obtained with a new set of parameters that fit r_s and N_{int} exactly in a non-perturbative calculation ($R = 0.409$ Bohr and $\alpha = 4.554$—see [7] for the corresponding perturbative parameters).

Property	Perturbative	Non-perturbative A	Non-perturbative B	Non-perturbative C
r_s (Bohr)	3.93	3.93	4.00	3.93
e (eV)	−6.22	−6.18	−6.18	−6.22
B (Mbar)	0.071	0.078	0.065	0.071
B'	3.6	3.5	3.6	3.9
$\bar{n}_{int}/\bar{n}$	1.066	1.032	1.024	1.066
$(\bar{n}/\bar{n}_{int})\ \mathrm{d}\bar{n}_{int}/\mathrm{d}\bar{n}$	1.182	1.156	1.164	1.165

are compared not only to experiment but also to those of two simple models: the stabilized jellium model [8] (a structureless precursor of our local pseudopotential) and the universal binding energy curve (UBEC) of Smith and co-workers [17]. Except for for Be, Pb and the alkaline earths, the local pseudopotential cohesive energies are realistic, and the UBEC emulates them rather well. The pseudopotential and all-electron ionization energies, excitation energies and valence densities have also been compared with one another. The

pseudopotential ionization energies are usually realistic. It is in the excitation energies of the free atom that the need for non-locality is most striking.

Table 3. Cohesive energies and average valence electron density parameters r_s^* for six-atom octahedral clusters. $r_s^* = 0.5527\,b/z^{1/3}$, where b is the nearest-neighbour bond length. The geometry is constrained to a regular octahedron. Local pseudopotential [7] and all-electron results are compared. Our calculations in tables 3 and 4 employ spin-polarized LSD for the atom, and spin-unpolarized LSD for the cluster. The all-electron results of [25], in parentheses, employ spin-polarized LSD for both. S is the total spin of cluster, from [25]. (Numerical values from the calculation of [25] have been provided by G S Painter, private communication.)

Cohesive energy (eV/atom)				
Cluster	(S)	Pseudopotential	All-electron	
Li_6	(1)	0.72	0.86	(0.88)
Na_6	(1)	0.53	0.63	(0.61)
Mg_6	(0)	0.17	0.22	(0.23)
Al_6	(1)	2.02	2.13	(2.12)
Density parameter r_s^* (Bohr)				
Cluster		Pseudopotential	All-electron	
Li_6		3.20	3.10	(3.05)
Na_6		3.80	3.60	(3.60)
Mg_6		2.98	2.86	(2.80)
Al_6		2.01	1.96	(2.01)
Self-compression ratio r_s^*/r_s (relative to bulk)				
Cluster		Pseudopotential	All-electron	
Li_6		0.99	0.99	(0.98)
Na_6		0.97	0.96	(0.96)
Mg_6		1.13	1.12	(1.10)
Al_6		0.98	0.96	(0.99)

The story that emerges from all these studies is consistent: our local pseudopotential provides a sort of average of the pseudopotentials experienced by s, p, d and f electrons in a more accurate non-local description, with the weights roughly optimized for the bulk solid. Transferred to another environment, it makes errors that can be corrected by making the potential more repulsive for s electrons and increasingly less repulsive for p, d and f electrons. In agreement with the conventional picture of non-locality, there is a strong splitting between the s and p potentials for Li and Be, due to the absence of p electrons from their cores. In Ca, the s–p splitting is weak, but there is a strong p–d splitting, due to the absence of d electrons from the core [18, 19]. Non-locality is most important for the elements Li, Be, Ca, Sr and Ba.

Our local pseudopotentials have been constructed systematically for all the simple metals. Originally intended for use in a perturbative description of a close-packed solid, they transfer to other chemical environments about as well as could be hoped.

2. Solid-state tests of transferability

Our local pseudopotentials, constructed in the solid state for the equilibrium lattice and lattice constant, have already been transferred successfully [7] to small changes of lattice constant under pressure (and to several close-packed crystal structures at the equilibrium

density). However, a successful prediction of the bulk modulus does not establish that the binding energy curve of the solid will be accurate over a wide range of lattice constants.

A key ingredient for the construction of the local pseudopotential is N_{int}, the number of valence electrons in the interstitial region between the surface of the polyhedral Wigner–Seitz cell and the largest inscribed sphere. Figure 2 shows the dependence of N_{int} upon r_s, the average valence electron density parameter, for body-centred-cubic (bcc) sodium, evaluated to first order in the pseudopotential via equation (2.17) of [7]. In the highly compressed limit $r_s \to 0$, N_{int} passes to its 'universal' value N_{int}^U appropriate to a uniform density of valence electrons, because the kinetic energy per electron overwhelms the pseudopotential. As r_s increases from 0, N_{int} first increases slightly (due to repulsion from the core) and then decreases again. At the equilibrium $r_s = 3.93$ Bohr, N_{int} is still not too different from its 'universal' value, so the first-order perturbation expansion is still valid. This expansion eventually breaks down as the crystal is expanded, predicting a negative N_{int} for large r_s where the exact N_{int} tends to zero from the positive side (the separated-atom limit).

Table 4. Cohesive energies and average valence electron density parameters r_s^* for dimers. See the caption of table 3.

Cohesive energy (eV/atom)				
Cluster	(S)	Pseudopotential	All-electron	
Li_2	(0)	0.52	0.52	(0.51)
Na_2	(0)	0.46	—	(0.44)
Mg_2	(0)	0.04	—	(0.09)
Density parameter r_s^* (Bohr)				
Cluster		Pseudopotential	All-electron	
Li_2		2.72	2.83	(2.84)
Na_2		3.19	—	(3.12)
Mg_2		3.15	—	(2.85)
Self-compression ratio r_s^*/r_s (relative to bulk)				
Cluster		Pseudopotential	All-electron	
Li_2		0.84	0.91	(0.90)
Na_2		0.81	—	(0.83)
Mg_2		1.19	—	(1.12)

As can be seen in figure 2 and in the caption of table 1, different crystal structures for the same element have roughly the same interstitial density $\bar{n}_{int} = N_{int}/\Omega_{int}$, but different interstitial volumes Ω_{int}.

In order to achieve good transferability to another lattice constant, the pseudopotential should predict the all-electron value of $\bar{n}_{int}$ for that lattice constant. Thus, a test of solid-state transferability is a comparison of the dimensionless parameter

$$\frac{\bar{n}}{\bar{n}_{int}} \frac{\mathrm{d}\bar{n}_{int}}{\mathrm{d}\bar{n}} = 1 - \frac{r_s}{3N_{int}} \frac{\mathrm{d}N_{int}}{\mathrm{d}r_s} \tag{2}$$

at the equilibrium r_s from pseudopotential and all-electron full-potential calculations. Table 1 shows such a comparison for all 16 simple metals, in which the pseudopotential result has been evaluated via first-order perturbation theory. This table suggests that the local pseudopotential is poorly transferable for Li, Be, Ca, Sr, Ba, Tl, Sn and Pb, where the pseudopotential makes large relative errors, and well or reasonably transferable for the other metals. This result was partly expected: Li and Be have highly non-local

pseudopotentials because they lack p electrons in the ionic core, so only s electrons experience a pseudopotential repulsion. Ca similarly lacks d electrons in the core, so only s and p electrons experience a pseudopotential repulsion. In all of the alkaline earths, the d component of the non-local pseudopotential is much more attractive than the s and p components, and is also strongly energy dependent due to the nearness to the Fermi level of low-lying empty d-state resonances [18, 19]. Thus, both non-locality and s–d hybridization are important in Ca, Sr and Ba. The heavier metals have relativistic effects which have been incorporated only through their influence on $\bar{n}_{int}$ at equilibrium.

Our solid-state construction, applications and tests rely upon a perturbation expansion of the density to first order and the total energy to second order in the pseudopotential. As already observed, this expansion cannot be used for a highly expanded lattice, or for a free atom or cluster. Thus, the accuracy of perturbation theory is, for us, a transferability issue. As a first step, we can define two dimensionless parameters that measure the strength of the perturbation. The first is $|e_{bs}|/e_F$, where e_{bs} is the second-order band-structure energy and e_F is the free-electron Fermi energy; this parameter ranges from 0.05 (Na) to 0.10 (Rb). The second is $\max_{G\neq 0}|w(G)/\Omega_0\epsilon(G)|/e_F$ where $w(G)$ is the Fourier transform of the pseudopotential evaluated at a non-zero reciprocal-lattice vector G, Ω_0 is the volume per atom, and $\epsilon(G)$ is the dielectric function; this parameter ranges from 0.08 (Al) to 0.11 (Pb).

As a test of the adequacy of perturbation theory, table 2 compares perturbative and non-perturbative results for sodium using our local pseudopotential. The non-perturbative results were obtained by diagonalizing large matrices in a plane-wave basis [20], and are converged with respect to basis set. For sodium our low-order expansion in powers of the pseudopotential is accurate, as others [21] have also found. This expansion is less reliable for polyvalent metals, such as magnesium and aluminium [21], although the fitting of the pseudopotential within perturbation theory yields good bulk moduli [7]. For use in a non-perturbative calculation, the parameters of our pseudopotential should ideally be readjusted to fit r_s and N_{int} in a non-perturbative solid-state calculation. Such new parameters for Na are indicated in table 2. In the remainder of this article, we use the original parameters from the perturbative fit of [7].

3. Cluster tests of transferability

Clusters stand midway between bulk metals and free atoms, and represent a potentially useful application of local pseudopotentials. In previous work [22, 23, 24], two of us have shown that macroscopic surface and curvature energies suffice to determine the 'smooth' (non-shell-structure) part of the total energy of a small cluster. Painter and Averill [25] have found that six-atom octahedral clusters of the elements exhibit many of the same trends across the periodic table as do the bulk solids. Such octahedra can be 'cut out' of the face-centred-cubic (fcc) lattice, with no distortion of bond angles, or out of the body-centred-cubic (bcc) or hexagonal-close-packed (hcp) lattice with some distortion.

As a test of the transferability of our local pseudopotential, we have compared pseudopotential and all-electron calculations of the cohesive energy per atom ϵ_{coh} and equilibrium nearest-neighbour distance b in the octahedral clusters Li_6, Na_6, Mg_6, and Al_6 (table 3). The nearest-neighbour distance in the cluster has been converted to an effective r_s^* using the relationship appropriate to an fcc crystal, $r_s^* = b\sqrt{2}(3/16\pi z)^{1/3}$. As expected, we find good agreement for ϵ_{coh} and r_s^*/r_s^B (where r_s^B is the bulk density parameter) for these metals.

Our pseudopotential [7] has been fitted to the *observed* r_s^B of the bulk solid, which the all-electron calculations underestimate by several per cent due to errors in the local density

Table 5. Cohesive energies for the mono- and divalent metals. Stabilized jellium (SJ) and local pseudopotential [7] results are compared to experiment [34]. Bulk solid calculations were done in second-order perturbation theory (except for SJ, which has no band structure), and pseudo-atom calculations were performed non-perturbatively.

Metal		Pseudo-atom energy (eV)	(error)	Cohesive energy (eV)	(error)	$\epsilon_{coh} = (16\pi/3) \times Br_s^3 z/(B'-1)^2$
Li	SJ	−6.28		1.16		
	Pseudopotential	−5.97	(+12%)	1.30	(−21%)	1.09
	Experiment	−5.32		1.65		
Na	SJ	−5.42		0.82		
	Pseudopotential	−5.21	(+1%)	1.01	(−9%)	0.99
	Experiment	−5.14		1.11		
K	SJ	−4.60		0.69		
	Pseudopotential	−4.36	(+0%)	0.81	(−13%)	0.83
	Experiment	−4.34		0.93		
Rb	SJ	−4.36		0.62		
	Pseudopotential	−4.15	(−1%)	0.73	(−13%)	0.78
	Experiment	−4.18		0.84		
Cs	SJ	−4.09		0.56		
	Pseudopotential	−3.90	(0%)	0.66	(−16%)	0.75
	Experiment	−3.89		0.79		
Be	SJ	−31.96		1.05		
	Pseudopotential	−31.57	(+15%)	0.87	(−74%)	2.07
	Experiment	−27.53		3.36		
Mg	SJ	−23.61		1.16		
	Pseudopotential	−23.06	(+2%)	1.19	(−22%)	1.63
	Experiment	−22.68		1.53		
Ca	SJ	−19.63		1.03		
	Pseudopotential	−18.84	(+5%)	1.22	(−34%)	1.66
	Experiment	−17.98		1.85		
Sr	SJ	−18.16		0.96		
	Pseudopotential	−17.42	(+4%)	1.15	(−32%)	1.59
	Experiment	−16.72		1.70		
Ba	SJ	−17.55		0.94		
	Pseudopotential	−16.89	(+11%)	1.06	(−43%)	1.42
	Experiment	−15.21		1.87		

approximation for exchange and correlation. For the all-electron values of r_s^B, we have used full-potential local spin-density values available in the literature: 3.14 Bohr for Li [26], 3.77 Bohr for Na [26], 2.55 Bohr for Mg [27], and 2.04 Bohr for Al [28].

For Li_6 and Na_6, $r_s^*/r_s^B < 1$ as predicted [29] by the stabilized jellium model [8, 22, 23, 24]: surface tension compresses the cluster, whether or not the gross shell structure of a spherical cluster is taken into account. But, for Al_6 $r_s^*/r_s^B \sim 1$, and for Mg_6 $r_s^*/r_s^B > 1$, as also found by Painter and Averill [25]. A possible explanation [25, 30] of this anomalous behaviour is that, with two electrons per unit cell, bulk Mg would be an insulator but for band overlap. With increasing cluster size, Mg is expected to pass over from van der Waals to metallic binding. If Mg_6 is much less strongly metallic than bulk Mg, then its weakened

Table 6. Cohesive energies for the tri- and tetravalent metals. See the caption of table 5.

Metal		Pseudo-atom energy (eV)	(error)	Cohesive energy (eV)	(error)	$\epsilon_{coh} = (16\pi/3) \times Br_s^3 z/(B'-1)^2$
Al	SJ	−53.56		3.73		
	Pseudopotential	−53.76	(+1%)	3.41	(+1%)	2.54
	Experiment	−53.26		3.38		
Ga	SJ	−50.87		3.73		
	Pseudopotential	−56.17	(−2%)	2.62	(−9%)	2.58
	Experiment	−57.22		2.87		
In	SJ	−46.95		3.32		
	Pseudopotential	−50.28	(−5%)	2.59	(+3%)	2.05
	Experiment	−52.68		2.52		
Tl	SJ	−45.68		3.35		
	Pseudopotential	−51.13	(−9%)	2.40	(+27%)	2.13
	Experiment	−56.36		1.89		
Sn	SJ	−80.15		4.74		
	Pseudopotential	−88.72	(−5%)	3.37	(+8%)	2.68
	Experiment	−93.21		3.13		
Pb	SJ	−77.67		4.62		
	Pseudopotential	−88.29	(−9%)	3.23	(+60%)	2.80
	Experiment	−96.70		2.02		

metallic bond could give rise to an expansion of the bond length.

Table 4 presents results for the dimers Li_2, Na_2, and Mg_2, which are still further removed from the solid-state origins of our local pseudopotential. (Unlike these three dimers, Al_2 is spin polarized and so has been omitted.) Except in sodium, the local pseudopotential predictions for the self-compression ratios r_s^*/r_s^B no longer provide such an accurate emulation of the all-electron predictions, although the cohesive energies are still accurate.

Our calculations for the six-atom clusters and dimers employ a linear-combination-of-atomic-orbitals local density molecular code [31]. Although the free atom is treated as spin polarized, the cluster or dimer is not. Neglect of spin polarization should have little effect on the nearest-neighbour distance of the six-atom spin-polarized clusters [29]; in any case, a fair test of pseudopotential transferability requires only that the pseudopotential and all-electron calculations be performed in the same way.

4. Atomic tests of transferability

As a test of transferability of our pseudopotential to the free atom, we have calculated the cohesive energies, some low-lying atomic excited states, the first ionization potentials and the radial valence electron densities, and have compared those quantities to all-electron and experimental results.

The cohesive energy is the difference between the energy of a free atom and the energy per atom of the bulk:

$$\epsilon_{coh} = z(e_{atom} - e). \tag{3}$$

In pseudopotential theory, e_{atom} is the energy per valence electron of the pseudo-atom

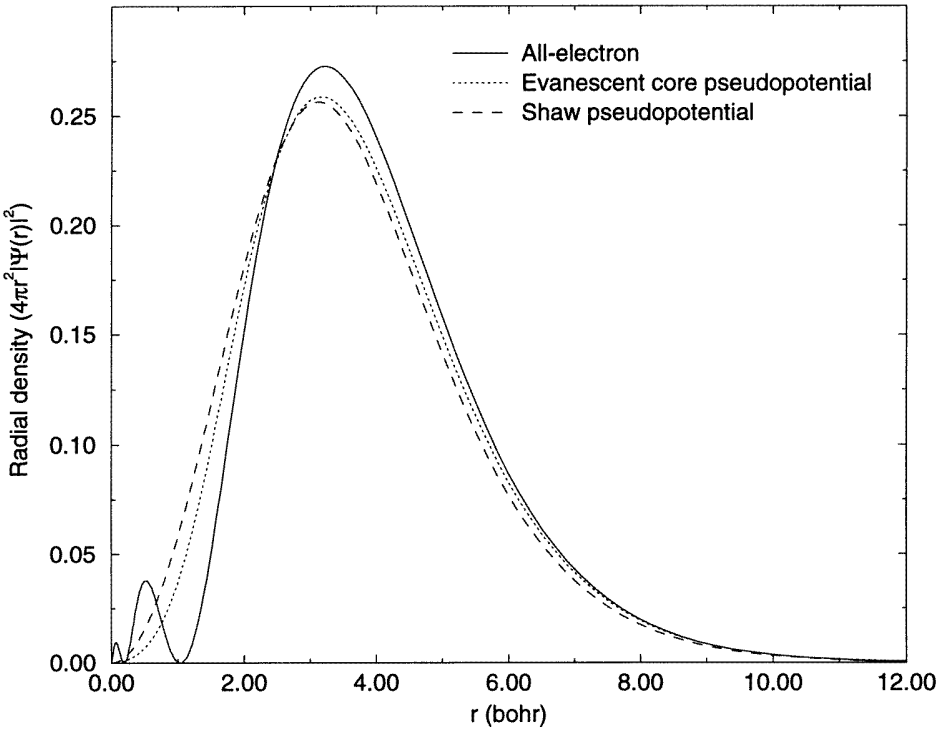

Figure 3. A comparison of the radial valence electron densities for the Na atom from an all-electron calculation and from the evanescent-core [7] and Shaw [36] local pseudopotentials.

(atomic valence electrons bound to an ionic core by the pseudopotential) and e is the binding energy per valence electron of the pseudo-solid (a sea of valence electrons bound to the lattice of ions by the same pseudopotential). The ground-state energy of the 16 pseudo-atoms was evaluated using the local spin-density approximation of Kohn–Sham density functional theory, with the correlation energy of [32]. This calculation was done using the Liberman, Cromer and Waber atomic code [33], but non-relativistically, as the pseudopotential (with parameters fitted to scalar-relativistic all-electron calculations) is supposed to provide some of the relativistic corrections. We have obtained the binding energy of the bulk solids using second-order perturbation theory (see section 2). Two different models of increasing sophistication were tested: stabilized jellium and the individual pseudopotential (see [7]).

We can directly compare the pseudo-atom energy with experiment, since it corresponds to the sum of the ionization energies of all valence electrons. As tables 5 and 6 show, our local pseudopotential achieves a remarkable agreement with experiment [34] for the alkalis (excepting Li), the alkaline earths (excepting Be) and even for the tri- and tetravalents. For the first two groups, the valence electrons are predicted to be a bit more bound than in experiment, while the opposite behaviour is found for the last two groups.

The cohesive energy, as shown in the same tables, improves systematically when we go from the structureless pseudopotential model (stabilized jellium [8]) to our structured local pseudopotential. The cohesive energy evaluated with the local pseudopotential is close to experiment in most cases. The biggest discrepancies are again for Li and Be, and also Ca, Sr, Ba and Pb. The cohesive energy of aluminium is very well described, probably

Table 7. Low-lying excitation energies for the atoms. All of the calculations were performed using the local spin-density approximation of Kohn–Sham theory. ΔE_{ae} is the all-electron excitation energy and ΔE_{ps} is the pseudo-atom excitation energy, obtained using the local pseudopotential of [7]. 'Ionization' stands for the first ionization energy evaluated as the difference between the total ground-state energies for the singly positive ion and the neutral atom. Excitation energies were calculated for all of the atoms, but some have been suppressed for the sake of brevity.

Metal	Excitation	ΔE_{ae} (eV)	ΔE_{ps} (eV)	(Error)
Li	$(2s\uparrow)^1 \rightarrow (2p\uparrow)^1$	1.82	2.80	(54%)
	$(2s\uparrow)^1 \rightarrow (3s\uparrow)^1$	3.27	3.65	(12%)
	$(2s\uparrow)^1 \rightarrow (3p\uparrow)^1$	3.73	4.49	(20%)
	$(2s\uparrow)^1 \rightarrow (3d\uparrow)^1$	3.91	4.42	(13%)
	$(2s\uparrow)^1 \rightarrow (4s\downarrow)^1$	4.80	5.17	(8%)
	Ionization $(2s\uparrow)$	5.47	5.97	(9%)
Na	$(3s\uparrow)^1 \rightarrow (3p\uparrow)^1$	2.19	2.20	(0%)
	$(3s\uparrow)^1 \rightarrow (4s\uparrow)^1$	3.19	3.06	(−4%)
	$(3s\uparrow)^1 \rightarrow (3d\uparrow)^1$	3.80	3.67	(−3%)
	$(3s\uparrow)^1 \rightarrow (4p\uparrow)^1$	3.87	3.81	(−2%)
	Ionization $(3s\uparrow)$	5.37	5.21	(−3%)
K	Ionization $(4s\uparrow)$	4.54	4.36	(−4%)
Rb	Ionization $(5s\uparrow)$	4.39	4.15	(−5%)
Cs	$(6s\uparrow)^1 \rightarrow (6p\uparrow)^1$	1.50	1.28	(−14%)
	$(6s\uparrow)^1 \rightarrow (5d\uparrow)^1$	1.76	2.39	(36%)
	$(6s\uparrow)^1 \rightarrow (7s\uparrow)^1$	2.34	2.10	(−10%)
	$(6s\uparrow)^1 \rightarrow (7p\uparrow)^1$	3.03	2.72	(−10%)
	Ionization $(6s\uparrow)$	4.08	3.90	(−5%)
Be	$(2s\uparrow)^1 \rightarrow (2p\downarrow)^1$	2.48	5.53	(123%)
	$(2s\uparrow)^1 \rightarrow (2p\uparrow)^1$	3.49	6.27	(80%)
	$(2s\uparrow)^1 \rightarrow (3s\downarrow)^1$	6.08	7.13	(17%)
	$(2s\uparrow)^1(2s\downarrow)^1 \rightarrow (2p\uparrow)^2$	6.12	13.33	(118%)
	$(2s\uparrow)^1 \rightarrow (3s\uparrow)^1$	6.24	7.36	(18%)
	Ionization $(2s\uparrow)$	9.04	10.36	(15%)
Mg	$(3s\uparrow)^1 \rightarrow (3p\downarrow)^1$	2.83	3.02	(7%)
	$(3s\uparrow)^1 \rightarrow (3p\uparrow)^1$	3.46	3.66	(6%)
	$(3s\uparrow)^1 \rightarrow (4s\downarrow)^1$	5.07	4.84	(−5%)
	$(3s\uparrow)^1 \rightarrow (4s\uparrow)^1$	5.19	5.03	(−3%)
	$(3s\uparrow)^1(3s\downarrow)^1 \rightarrow (3p\uparrow)^2$	6.64	7.29	(10%)
	Ionization $(3s\uparrow)$	7.75	7.61	(−2%)

due to a cancellation between the local-density-approximation error and the pseudopotential error. The local density approximation is known to overestimate the cohesive energy of the non-alkali metals [35]. We find such overestimation for Al, In, Tl, Sn and Pb.

It is interesting to track the origin of the errors in the cohesive energy. For the alkalis, our very good description of the pseudo-atom energy suggests that any error in the cohesive energy comes mainly from the solid. For the alkaline earths, the main error seems to come from the atom. Nevertheless, for Ca, Sr and Ba, the solid-state sd-hybridization contributions to the energy found by Moriarty [19] could bring our cohesive energies into agreement with experiment. For the $z = 3$ group, the errors in the pseudo-atom and in the solid tend to compensate each other, and the same can be said, although to a lesser extent,

Table 8. See the caption of table 7.

Metal	Excitation	ΔE_{ae} (eV)	ΔE_{ps} (eV)	(Error)
Ca	$(4s\uparrow)^1 \rightarrow (3d\downarrow)^1$	1.81	4.39	(142%)
	$(4s\uparrow)^1 \rightarrow (4p\downarrow)^1$	2.01	1.99	(−1%)
	$(4s\uparrow)^1 \rightarrow (3d\uparrow)^1$	2.17	4.53	(109%)
	$(4s\uparrow)^1 \rightarrow (4p\uparrow)^1$	2.45	2.54	(4%)
	$(4s\uparrow)^1 \rightarrow (5s\downarrow)^1$	3.93	3.75	(−5%)
	Ionization $(4s\uparrow)$	6.25	6.24	(−0%)
Sr	Ionization $(5s\uparrow)$	5.87	5.78	(−2%)
Ba	Ionization $(6s\uparrow)$	5.37	5.60	(4%)
Al	$(3p\uparrow)^1 \rightarrow (4s\downarrow)^1$	3.02	2.33	(−23%)
	$(3s\uparrow)^1(3p\uparrow)^1 \rightarrow (3p\downarrow)^2$	3.65	4.33	(18%)
	$(3p\uparrow)^1 \rightarrow (4p\uparrow)^1$	3.89	3.36	(−14%)
	$(3p\uparrow)^1 \rightarrow (3d\uparrow)^1$	4.10	3.61	(−12%)
	$(3p\uparrow)^1 \rightarrow (5s\uparrow)^1$	4.69	4.01	(−15%)
	Ionization $(3p\uparrow)$	5.98	5.38	(−10%)
Ga	Ionization $(4p\uparrow)$	6.01	5.27	(−12%)
In	Ionization $(5p\uparrow)$	5.69	5.13	(−10%)
Tl	Ionization $(6p\uparrow)$	5.49	5.03	(−8%)
Sn	Ionization $(5p\uparrow)$	7.40	6.80	(−8%)
Pb	$(6p\uparrow)^1 \rightarrow (6p\downarrow)^1$	0.45	0.51	(13%)
	$(6p\uparrow)^1 \rightarrow (7s\uparrow)^1$	3.78	3.29	(−13%)
	$(6p\uparrow)^1 \rightarrow (7s\downarrow)^1$	3.90	3.44	(−12%)
	$(6p\uparrow)^1 \rightarrow (7p\uparrow)^1$	4.98	4.54	(−9%)
	$(6p\uparrow)^2 \rightarrow (6p\downarrow)^1(7p\uparrow)^1$	5.03	4.60	(−8%)
	Ionization $(6p\uparrow)$	7.10	6.69	(−6%)

for $z = 4$.

We have not attempted to evaluate all-electron cohesive energies, which are typically small differences between large total energies and thus require careful balancing of the errors in the atomic and solid-state codes.

From the universal binding energy curve (UBEC) of Smith and co-workers [17], we extract the following relationship involving ϵ_{coh}, B, and B':

$$\epsilon_{coh} = 4z \left(\frac{\partial^2 e}{\partial r_s^2}\right)^3 \Bigg/ \left(\frac{\partial^3 e}{\partial r_s^3}\right)^2 = \frac{16\pi}{3} \frac{B r_s^3 z}{(B'-1)^2}. \tag{4}$$

This relation also follows directly from (2.5), (2.15) and the line below equation (2.13) in [17c]. As a test of this relationship (and, therefore, of the UBEC), we have used our calculated B and B' from [7] in the right-hand side of equation (4) and compared with the cohesive energy calculated from equation (3), and with the experimental value [34]. Tables 5 and 6 demonstrate the good predictive power of the UBEC relationship.

Tables 7 and 8 show some low-lying excitation energies and the first ionization potential obtained in a local spin-density description of the atom. Again the excitation and ionization energies were evaluated non-relativistically for the pseudopotential case and relativistically for the all-electron case. The agreement between the all-electron and pseudopotential results is good for the monovalent metals other than Li. Li, which has strong pseudopotential non-

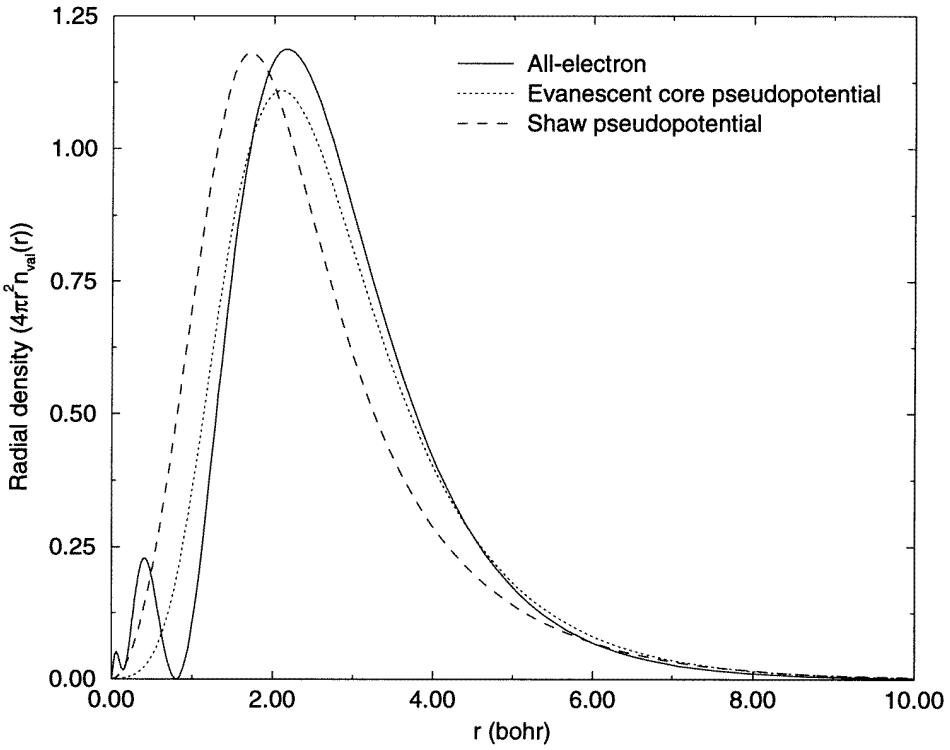

Figure 4. A comparison of the radial valence electron densities for the Al atom from an all-electron calculation and from the evanescent-core [7] and Shaw [36] local pseudopotentials.

locality, exhibits large errors for the sp transitions. The first excited state of Na comes out with exactly the right energy, while Cs displays a large error for an sd transition. Passing to the divalents, we find that Be has the same problems as Li, with sp transitions showing even bigger errors. Mg has acceptable transferability. For Ca, Sr, and Ba, large errors are found for the sd excitations. Our energy errors for sd transitions are always positive, showing that we need less repulsion for d states. For the tri- and tetravalent metals, the agreement between all-electron and local pseudopotential results is fair, with pp, sp and pd excitations showing errors of roughly the same size.

Ionization energies, obtained by stripping the atom of its outermost valence electron, are also in good agreement with all-electron results (and, therefore, with experiment). Even for Li and Be the agreement is satisfactory, although a bit worse than that obtained for the other metals of the same valence.

Good non-local pseudopotentials, with atomic orbital pseudo-densities fitted to all-electron orbital densities beyond a given core radius (norm-conserving pseudopotentials), show very small errors in the low-lying energy spectrum [16]. To understand the larger local pseudopotential errors in tables 7 and 8, we have plotted in figure 3 the valence electron radial densities, both in the all-electron and in the local pseudopotential case, using the local spin-density approximation. For Na, the agreement between these densities is reasonable beyond the radial distance $r \sim r_{WS} = r_s$, although not so perfect as for norm-conserving pseudopotentials. Since our pseudopotential is less repulsive than the s component of a good non-local pseudopotential (such as Hamann's [15]) near the conventional core radius,

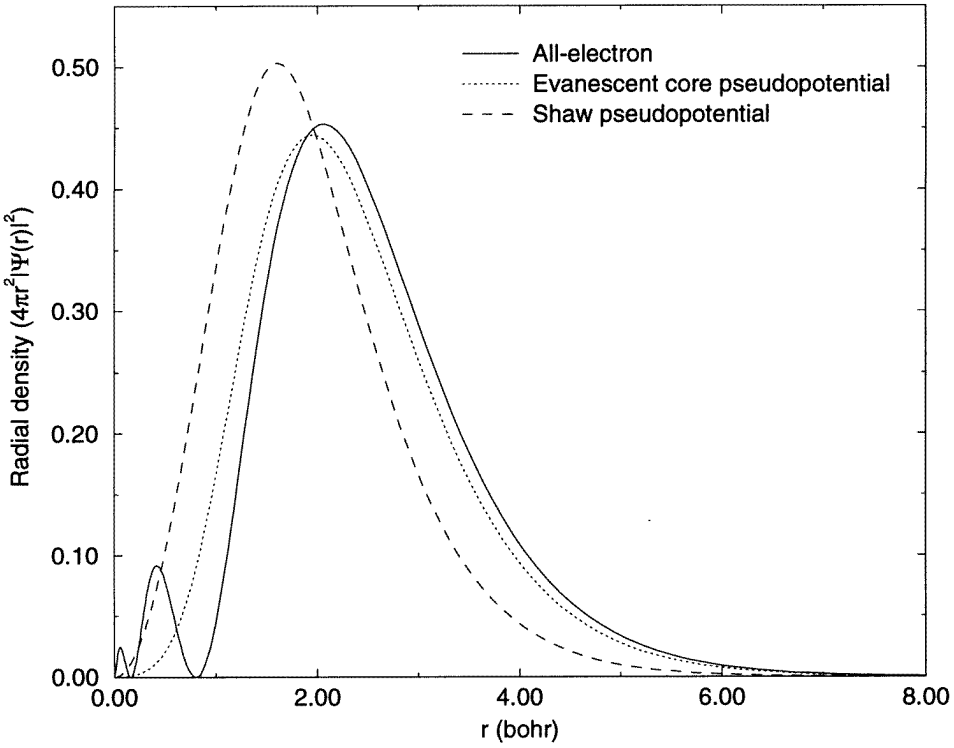

Figure 5. A comparison of the s parts of the radial valence electron densities for the Al atom. See the caption of figure 4.

our electron density is slightly shifted inwards.

In figures 4–6 the radial valence electron density for the Al pseudo-atom is plotted against the all-electron result, showing both the total valence electron density and its separate s and p contributions. Although the total valence charge densities of the all-electron and pseudopotential calculations are similar for distances $r \geqslant r_{WS}$, examination of the s and p charge densities shows that the former is underestimated in the pseudo-atom while the latter is overestimated for that range of distances. This limitation of our local pseudopotential follows from its very construction: the potential is fitted to the total valence electron density of the solid, and not to the individual atomic states of the polyvalents.

Figures 3–6 also show the atomic density obtained from the local Shaw pseudopotential (figure 1 and [36]) with its one parameter fitted [13] to the equilibrium valence electron density of the solid. As expected from arguments in [37] and [38], our local pseudopotential with its harder core transfers better to the atom than does the Shaw form. Modelling an ion as a rigid sphere of stabilized jellium [8] or ideal metal [10] leads to a soft-core pseudopotential not unlike the Shaw form, and with the same limitations. Harder cores are more transferable, although solid-state calculations using them require more plane waves and higher orders of perturbation theory. Increasing the nominal valence z for a given element would also improve transferability and would extend local pseudopotentials to the whole periodic table [39], but at a still greater computational cost.

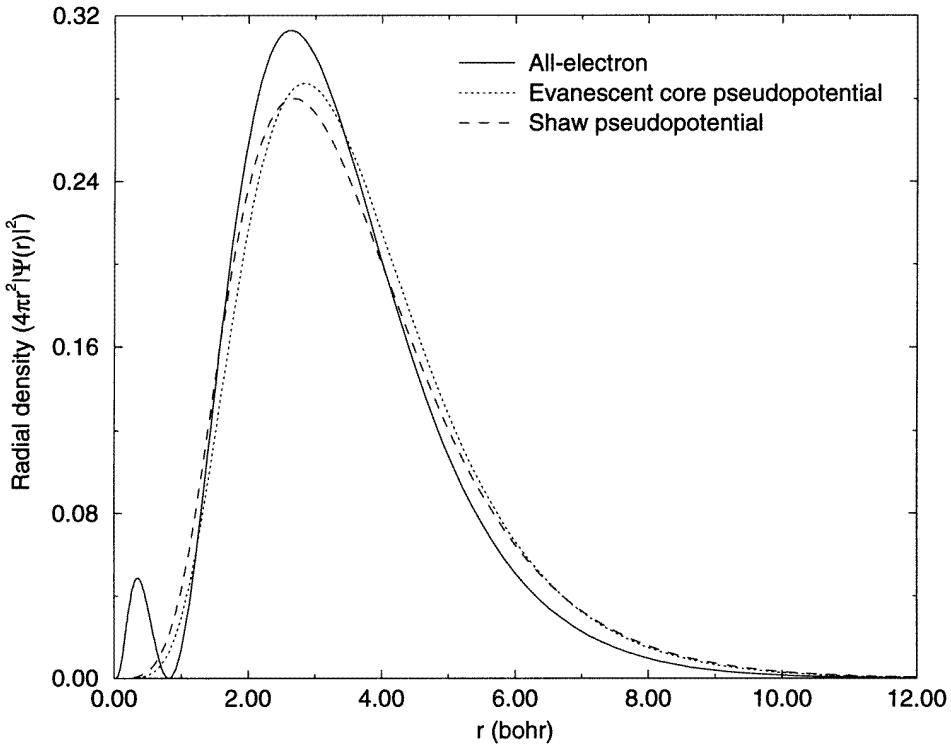

Figure 6. A comparison of the p parts of the radial valence electron densities for the Al atom. See the caption of figure 4.

Acknowledgments

We thank John Smith, Gayle Painter, Weitao Yang, José Luís Martins and Michael Teter for helpful discussions and information. This work was supported in part by a NATO collaborative research grant, and in part by the US National Science Foundation under Grant No DMR92-13755.

References

[1] Harrison W A 1966 *Pseudopotentials in the Theory of Metals* (New York: Benjamin)
[2] Cohen M L 1994 *Solid State Commun.* **92** 45
[3] Pickett W E 1989 *Comput. Phys. Rep.* **9** 117
[4] Payne M C, Teter M P, Allan D C, Arias T A and Joannopolous J D 1992 *Rev. Mod. Phys.* **64** 1045
[5] Dreizler R M and Gross E K U 1990 *Density Functional Theory* (Berlin: Springer)
[6] Bylander D M, Gu Y M and Kleinman L 1995 *Phys. Rev.* B **51** 2566
[7] Fiolhais C, Perdew J P, Armster S Q, MacLaren J M and Brajczewska M 1995 *Phys. Rev.* B **51** 14 001
The pseudopotential parameters and calculated properties are very slightly in error due to inadvertent use of the exchange-only local field correction, which omits correlation. In the present work, we have used corrected pseudopotential parameters from an erratum submitted to *Phys. Rev.* B.
[8] Perdew J P, Tran H Q and Smith E D 1990 *Phys. Rev.* B **42** 11 627
[9] Wojciechowski K F 1995 *Phys. Rev.* B **51** 2563
[10] Rose J H and Shore H B 1994 *Phys. Rev.* B **49** 11 588; 1993 *Phys. Rev.* B **48** 18 254
[11] Ashcroft N W 1966 *Phys. Lett.* **23** 48

[12] Hasegawa M and Young W H 1981 *J. Phys. F: Met. Phys.* **11** 977
[13] Ling D D and Gelatt C D 1980 *Phys. Rev.* B **22** 557
[14] Moriarty J A 1977 *Phys. Rev.* B **16** 2537
[15] Hamann D R 1989 *Phys. Rev.* B **40** 2980
[16] Teter M 1993 *Phys. Rev.* B **48** 5031
[17] (a) Rose J H, Ferrante J and Smith J R 1981 *Phys. Rev. Lett.* **47** 675
(b) Rose J H, Smith J R, Guinea F and Ferrante J 1984 *Phys. Rev.* B **29** 2963
(c) Vinet P, Rose J H, Ferrante J and Smith J R 1989 *J. Phys.: Condens. Matter* **1** 1941
[18] Dagens L, Rasolt M and Taylor R 1975 *Phys. Rev.* B **11** 2726
[19] Moriarty J A 1979 *Phys. Rev.* B **19** 609
[20] Ihm J, Zunger A and Cohen M L 1979 *J. Phys. C: Solid State Phys.* **12** 4409
[21] Brovman E G, Kagan Y and Kholas A 1972 *Sov. Phys.–JETP* **34** 344
Bertoni C M, Bortolani V, Calandra C and Nizzoli F 1974 *J. Phys. F: Met. Phys.* **4** 19
Benckert S 1975 *Phys. Status Solidi* b **69** 483
[22] Fiolhais C and Perdew J P 1992 *Phys. Rev.* B **45** 6207
[23] Brajczewska M, Fiolhais C and Perdew J P 1993 *Int. J. Quantum Chem.* S **27** 249
[24] Ziesche P, Perdew J P and Fiolhais C 1994 *Phys. Rev.* B **49** 7916; 1994 *Phys. Rev.* B **50** 5020
[25] Painter G S and Averill F W 1994 *Phys. Rev.* B **50** 5545
[26] Sigalas M, Bacalis N C, Papaconstantopoulos D A, Mehl M J and Switendick A C 1990 *Phys. Rev.* B **42** 11 637
[27] Juan Y-M and Kaxiras E 1993 *Phys. Rev.* B **48** 14 944
(Nonlocal pseudopotential results for Mg, where full-potential all-electron results were unavailable.)
[28] Dufek P, Blaha P and Schwarz K 1994 *Phys. Rev.* B **50** 7279
[29] Perdew J P, Brajczewska M and Fiolhais C 1993 *Solid State Commun.* **88** 795
[30] Pastor G M and Bennemann K H 1994 *Clusters of Atoms and Molecules* ed H Haberland (Berlin: Springer)
[31] Yang W 1991 *Phys. Rev.* A **44** 7823
[32] Perdew J and Zunger A 1981 *Phys. Rev.* B **23** 5048
[33] Liberman D A, Cromer D T and Waber J T 1971 *Comput. Phys. Commun.* **2** 107, 471; 1975 *Comput. Phys. Commun.* **9** 129
[34] Emsley J 1991 *The Elements* (Oxford: Clarendon)
[35] Jones R O and Gunnarsson O 1989 *Rev. Mod. Phys.* **61** 689
[36] Shaw R W 1968 *Phys. Rev.* **174** 769
[37] Harris J and Jones R O 1978 *Phys. Rev. Lett.* **41** 191
[38] Goedecker S and Maschke K 1992 *Phys. Rev.* A **45** 88
[39] Starkloff T and Joannopoulos J D 1977 *Phys. Rev.* B **16** 5212